Brain Tumour Segmentation with Quantitative MRI

S. Wildenburg[1], H. Neeb[1], N. J. Shah[1]

[1]Institute of Medicine, Forschungszentrum Jülich, Jülich, Germany

INTRODUCTION

One of the challenges met in brain tumour diagnostics is associated with the precise separation between tumour and normal healthy tissue for biopsies and anti-cancer therapy. We present a new method for tumour tissue segmentation based on extensions to multivariate clustering analysis of quantitative T_1, T_2^* and H_2O content maps acquired with MRI. Additional parameters that are sensitive to the local magnetic field offset were also included in the segmentation algorithm. First results from a current clinical study for the differentiation of tumour, oedema, and surrounding healthy tissue are shown. Based on the high precision of the new MR measurement sequences in combination with the precise segmentation process and a total measurement time of approximately 21 minutes, the presented method demonstrates its relevance for possible use in clinical studies as well as routine diagnosis.

METHODS

T_2^* was measured using the QUTE-EPI sequence with the following parameters [1]: TR=138ms; TE=4ms; α=90°; 17 slices; 64 time points; echo spacing=2ms; matrix size=256^2; FOV=220mm; slice thickness=5mm; rf-spoiling employed; 10 preparation scans. T_1 mapping was performed using TAPIR [2]. The following parameters were employed: TR=15ms; TE_1: TE_2: TE_3=2.8: 5.1: 7.5ms; α=25°; 18 slices; 20 time points; matrix size=256^2; FOV=220mm; slice thickness=5mm; sequential excitation; delay time τ=2s. The first point for the first slice on the recovery curve was sampled 10ms after inversion. Inefficiencies of the inversion pulse were corrected using the procedure described in [3]. Quantitative H_2O content was determined by the method described in [5][6]. In order to perform quantitative H_2O content mapping in regions of large field inhomgeneities, the signal decay curve was fitted with a 3rd order polynomial function and the fit was constraint to a number, N_p, of measured points [6]. The linear slope α_1 extracted from the polynomial fit and N_p were used as additional variables for the multivariate image segmentation process. In addition, the mean absolute deviation of the measured signal decay curve R_{Mean} from an exponential fit to the measured points was included in the clustering process. R_{Mean} is large in regions with large field inhomogeneities or significant bi-exponential signal behaviour.

Image segmentation is based on an extension to standard clustering approach termed Zoom-In-Clustering. Zoom-In-Clustering is based on the interactive and iterative combination of conventional clustering algorithms like k-Means or Complete-Linkage. During the first step, clustering is performed for a given number $N_{c,1}$ of clusters. $N_{c,1}$ is either externally given or based on the Sum of Squares Within (SSW) criterion [7]. Depending on the results obtained it is possible to either stop the process or to define one or more clusters 1..k (k< $N_{c,1}$) that should be re-clustered again in a second step. The second step includes the same conventional clustering algorithm as before but works only on a subset of points (the "zoom-in" region) which where assigned previously to one of the clusters 1..k. The number of clusters in the second step $N_{c,2}$ is again either externally given or automatically extracted from the SSW criterion. In this case, the Sum of Squares Within will be determined based only on the points used for clustering in the second step. In addition, variables different from the ones used in the first step can be used for clustering. This offers the advantage of including variables known to be only sensitive or specific within the sub-region to be re-clustered again. The whole process can be repeated as many times as desired.

Clusters defined by this approach were solely determined by the quantitative MR parameter patterns without taking the spatial distribution of the resulting cluster structure into account. In order to check the spatial homogeneity of the resulting cluster structure, the weighted mean entropy <H> for each slice was calculated taking the different number of points assigned to different clusters into account:

$$< H >= \frac{\sum_{i=1}^{M} (M - k_{Ci}) H_i(P)}{\sum_{i=1}^{M} (M - k_{Ci})}.$$

Here, k_{Ci} is the number of points assigned to cluster C_i and M represents the total number of clustered points. H_i (P) is the entropy for voxel i and P=(p_1,…p_N) is the distribution of clusters in a 3x3 matrix of points surrounding the respective voxel.

Quantitative measurement of all the described parameters was performed in a 28 year old patient with oligodendroglioma in the frontal area. Two-step Zoom-In-Clustering based on both k-Means and Complete-Linkage was performed with $N_{c,1}$=5 and $N_{c,2}$=5 in a region comprising 2 clusters where tumour and oedema were identified. Water content, T_1 and T_2^* were used for the first clustering step and were extended by R_{Mean}, N_p and α_1 for the second step. The slice-dependent entropy was determined and compared with <H> obtained by conventional one-way k-Means and Complete-Linkage clustering.

RESULTS AND DISCUSSION

The slice dependence of the weighted mean entropy <H> is shown in Fig. 1a for the different approaches. k-Means results in a larger <H> compared to the Complete-Linkage algorithm for both conventional and Zoom-In-Clustering. Zoom-in-Clustering results in a more coherent cluster structure compared to the conventional approach. Fig. 1b shows the cluster maps resulting from the first step of Zoom-In Clustering. The tumourous region is well identified but partly overlapping with other brain structures. The overlap reduces when zooming into the yellow and light green region as shown in Fig 3b and tumour sub-structure becomes visible. The results shown demonstrate the clinical relevance of quantitative imaging in combination with the described Zoom-In clustering approach. Zoom-In clustering offers clear advantages compared to conventional One-Way clustering as it results in spatially more homogeneous segmentations. In addition, tumour substructures could be clearly and significantly identified in a patient suffering form an oligodendroglioma. The comparison between identified clusters and results obtained from histology is part of an upcoming clinical study based on the presented methods.

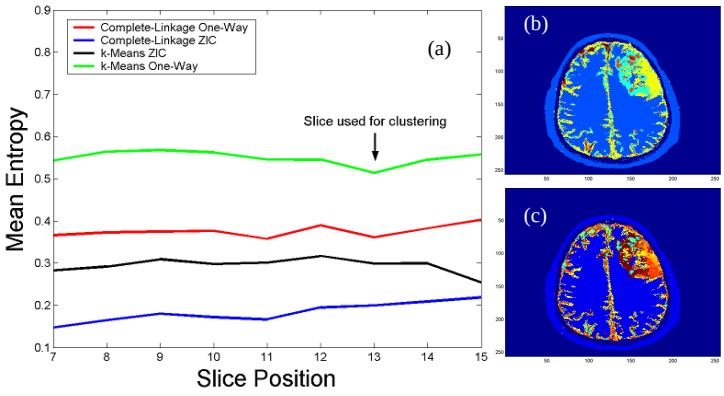

Fig 1: (a) Slice dependent weighted mean entropy for different clustering approaches. (b) Results from the first clustering step of Zoom-in-Clustering with $N_{c,1}$=5. (c) same as in (b) but after Zoom-In clustering with $N_{c,2}$=5.

REFERENCES

[1] Dierkes T et al., ICS 2004;**1265**:181-185.
[2] Steinhoff S et al., MAGN. RESON. MED. 2001;**46(1)**:131-140.
[3] Shah NJ et al., NEUROIMAGE 2001;**14**:1175-1185.
[4] Zaitsev et al., Magn. Reson. Med. 2003;**49(6)**:1121-1132.
[5] Neeb H et al., ICS 2004;**1265**:113-123.
[6] Neeb H et al., 2004, in preparation.
[7] Brian S. Everitt, "Cluster Analysis"; Third Edition; Jon Wiley and Sons Inc. 1993.